Supercontinuum ultra-high resolution line-field OCT; experimental spectrograph comparison and comparison with current clinical OCT systems by the imaging of a human cornea

Samuel Lawman[a,b], Vito Romano[b], Peter W. Madden[b], Sharon Mason[b], Bryan M. Williams[b], Yalin Zheng[b], Yao-Chun Shen*[a]

[a] Department of Electrical Engineering and Electronics, University of Liverpool, Liverpool L69 3GJ, UK; [b] Department of Eye and Vision Science, University of Liverpool, Liverpool L7 8TX, UK

*Y.C.Shen@liverpool.ac.uk; phone +44 (0)151 794 4575

ABSTRACT

Ultra high axial resolution (UHR) was demonstrated early in the development of optical coherence tomography (OCT), but has not yet reached clinical practice. We present the combination of supercontinuum light source and line field (LF-) OCT as a technical and economical route to get UHR-OCT into clinic and other OCT application areas. We directly compare images of a human donor cornea taken with low and high resolution current generation clinical OCT systems with UHR-LF-OCT. These images highlight the massive information increase of UHR-OCT. Application to pharmaceutical pellets, and the functionality and imaging performance of different imaging spectrograph choices for LF-OCT are also demonstrated.

Keywords: optical coherence tomography, ultra-high resolution, image segmentation, supercontinuum, cornea, pharmaceuticals

1. INTRODUCTION

Since the genesis paper in 1991[1] and the first commercial instrument 5 years later in 1996[2], Optical Coherence Tomography (OCT) has become standard in secondary care ophthalmology clinics, as well as finding applications in multiple areas of medicine[3] and beyond[4]. The term "ultra-high" resolution (UHR) is not definitively defined, but here we will define the boundary as an axial resolution less than 3 n_G.µm. An UHR system for *in vivo* tadpole measurements was described in 1999[5]. However, despite UHR systems being developed and used in research, no commercial clinical UHR system has successfully entered the market 18 years later. The higher resolution from UHR systems allows finer structures to be resolved and measured, increasing the diagnostic potential. Currently, corneal OCT is generally used in clinics for mapping the shape of the cornea and its thick layers (i.e. epithelium and stroma), and visualising wounds. UHR resolution would allow thin layers and finer details to be imaged as well, with the increased diagnostic potential of this having been evaluated for multiple conditions[6,7]. Likewise outside of medicine, UHR-OCT can be used to resolve even thinner structural layers, which could expand OCT's relevance in areas such as the quality assurance of coatings structures applied to pharmaceutical tablets[8] and pellets[9].

One reason for the absence of commercial clinical UHR-OCT systems is the cost of spatial coherent broad bandwidth light source suitable for the scanning point format of all current clinical OCT systems. Though the need for spatial coherence can be overcome with a time domain full field format allowing the use of cheap thermal source[10], these devices have not emerged clinically due to practical disadvantages compared with current Fourier domain scanning point systems. For commercial systems, two different types of light sources are currently used. Superluminescent diodes (SLDs) are used in spectral domain systems, however single SLDs are low bandwidth. Composite SLD sources can give more bandwidth, at a significantly higher cost, to just meet our definition of UHR[6]. Swept sources lasers are used in swept source OCT systems. Though these give benefits in terms of signal-to-noise ratio (SNR) and potential image depth[11], they currently do not have the bandwidth for UHR-OCT. One light source used for human *in vivo* UHR-OCT studies is femtosecond pulsed Ti:Saphire lasers[7], which give broad bandwidth, single spatial mode and very low spectral noise between pulses. However, they are very expensive making them uneconomical for commercial systems. Suppercontinuum light sources[12] use non-linear optics, generally in specially designed optical fibres, to significantly broaden the spectral output of laser sources. This technology is much cheaper than femtosecond lasers and turnkey commercial products give a single spatial mode output from 450 nm to 2000 nm, meaning the light source is no longer

the bandwidth limiting factor. As such, it has been used for corneal *in vivo* UHR-OCT[13]. Though continuous wave supercontinuum generation is feasible[14], the light sources currently available for OCT are pulsed with durations ranging from nanosecond to femtoseconds. Due to the stochastic nature of some of the non-linear processes involved, supercontinuum light sources suffer from spectral relative intensity noise (RIN), which for pulsed sources is noise in the spectrum between each pulse. Figure 1 shows example spectrum and SNR measurements for the physical averaging of different numbers of supercontinuum pulses. The method involved using neutral density filters to keep detection amplitude, thus shot and read noise, approximately equal for all measurements. The spectral RIN is large for the single pulse but reduces with the averaging of pulses. In this case, by 1000 pulses the SNR is starting to plateau and shot noise will be starting to dominate the measurement. RIN in the measured spectra translates to noise in an OCT A-Scan. Conventional scanning point OCT systems measure one A-Scan at a time, so to reduce supercontinuum RIN noise more pulses are needed to be averaged for each one. However, for faster image collection the A-Scan integration time, so averaged pulses, needs to be reduced, thus RIN may become significant source of noise for supercontinuum based OCT systems.

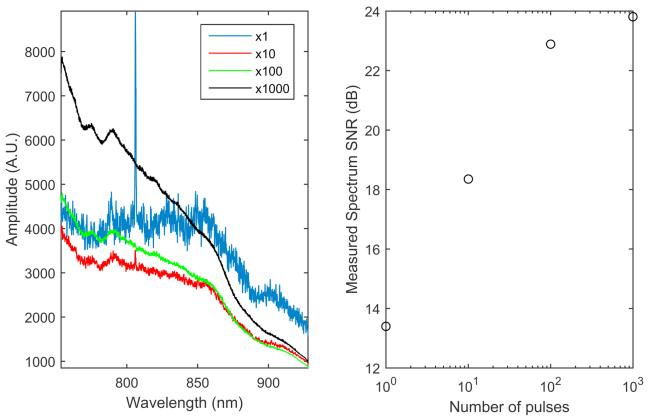

Figure 1. (Left) Example spectrums and (Right) spectrum temporal SNR measurements of different number of pulses from a supercontinuum source (NKT COMPACT).

Instead of measuring one A-Scan at a time, line field spectral domain (LF-) OCT[15,16] parallelises the measurement measuring a B-scan in a single shot with no moving parts. As many A-scans are measured at once, the A-scan integration time (number of pulses) is substantially increased compared to a conventional scanning point system operating at the same imaging speed, significantly reducing the RIN noise. In addition, with simultaneous capture of all A-Scans in a B-Scan, the spectrum RIN for each A-Scan is identical, meaning that the noise in each A-Scan is identical and thus fixed pattern, so can be mathematically recovered and removed from the image[15]. In our previous work[14], we demonstrated this for a B-Scan image taken with a single supercontinuum pulse. Due to the low cost bandwidth and RIN induced noise reduction; the combination of LF and supercontinuum light sources is a natural solution for commercial clinical or non-medical, as well as laboratory research, UHR-OCT systems.

Compared with conventional scanning point OCT systems, the removal of one dimension of the confocal gate in LF-OCT means that light that is not perfectly optically controlled, i.e. any source of aberrations including defocus, can be incident on adjacent parallel detector channels (A-Scans). As will be demonstrated, this optical cross-talk can cause image artefacts for certain samples. Particularly for research instruments, a key design choice for a LF-OCT is the imaging spectrograph setup. Commercial Czerny-Turner systems have been used particularly for demonstration of different LF-OCT setups[15,16]. The reflective optics and motorised interchangeable and adjustable grating mountings gives excellent flexibility at a click of the mouse, allowing different bandwidths (i.e. axial imaging ranges and resolutions) and central wavelengths to be chosen to suit the given experiment or changed during an experiment. However, the reflective optics of these spectrographs are not great imaging systems, suffering particularly from astigmatism. To overcome this, one option is the correction of the Czerny-Turner optics with a Schmidt plate[17], maintaining the flexibility of the Czerny-Turner spectrograph but removing optical aberrations/defocus. However, Schmidt-Czerny-Turner spectrographs are significantly more expensive and bulky than Czerny-Turner ones. To reduce size and cost, custom built refractive spectrographs with fixed gratings can be used[18,19] in LF-OCT systems. These reduce the flexibility potential, particularly to switch resolution and imaging depths, of the given OCT system but generally perform better optically. Experimental

evaluation of relative LF-OCT imaging performance of the three spectrograph designs has not previously been published.

In addition to medical instruments, an economical and practical UHR-OCT format also has the same benefits for other applications. Here we will also demonstrate images of multicoated pharmaceutical pellets taken with UHR-LF-OCT.

2. METHODS

2.1 Line field spectral domain OCT

The core LF-OCT system has been described previously[16], though in parts (section 2.2) of this work alternative imaging spectrographs are used. Figure 2 shows the set up of the LF-OCT interferometer. The suppercontinuum light source used in this work was the low cost Fianium Whitelase Micro, which provides low energy pulses at a fixed high (20 MHz) repetition rate. In this work the slow (physical shutter limited minimum exposure time of 60 ms) CCD cameras, with the light source power appropriately physically attenuated, were used. This meant each A-Scan was the average of 1.2 million pulses, making the effect of spectral noise negligible. For a setup suitable for *in vivo* measurements, using the fast (Andor Neo) camera with 1 ms exposure would give averaging of 20,000 pulses per A-scan.

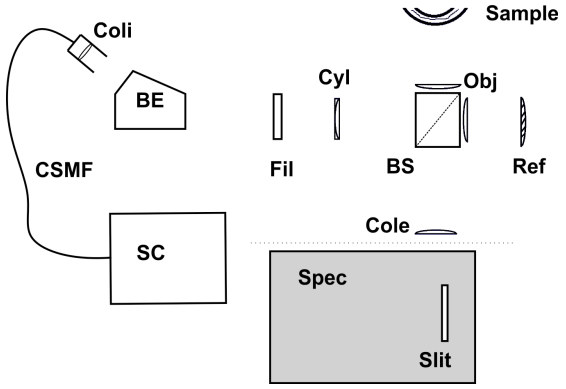

Figure 2. The LF-OCT apparatus format used in this study. SC - Super-Continuum light source, CSMF – Continuously Single Mode Fibre. Coli – Collimator, BE – Beam Expander, Fil – Optical Filters (Bandpass and Neutral Density), Cyl – Cylindrical Lens, BS – Cube Beam Splitter. Obj – Objective Lenses, Ref – Reference Interface (Flat glass surface), Cole – Collection Lens, Slit – Slit of imaging spectrograph which the line field spectral interferograms is imaged onto, Spec – One of three (describe in section 3.2) imaging spectrographs with 2D cameras to resolve the spectral interferogram.

2.2 Spectrograph evaluation

To evaluate the effect of three types of spectrograph (Czerny-Turner, Schmidt-Czerny-Turner and transmission) on the image quality of the LF-OCT images, the LF-OCT interferometer was setup with commercial spectrographs of the three types. These commercial systems can be regarded as near ideal constructions of their design. The three spectrograph systems were: the Andor shamrock 303i with Andor iVac camera and was used in the rest of this paper (Czerny-Turner), Princeton IsoPlane 320 with Princeton Pixis 400 camera (Schmidt-Czerny-Turner), and Andor Holospec with Andor iVac (transmission). To compare the setups, images of two artefact prone samples, curved cling film and optical lenses, and a fixed human donor cornea were compared. We have previously shown that a Fourier phase differential mask (FPDM) can be used to reduce aberration artefacts[16], the qualitative relative effect of this processing will also be compared.

2.3 Human donor cornea imaging, comparison of UHR-LF-OCT with current clinical OCT instruments

To compare the performance of UHR-LF-OCT with current commercial clinical systems, a human donor cornea was supplied from the Fondazione Banca Degli Occhi del Veneto Eye Bank after approval from University of Liverpool research ethics committee. So that it was of typical *in vivo* thickness, the cornea was supplied in a de-swelling solution (Modified E-MEM with 6% dextran T-500). For all measurements the cornea was mounted on an artificial anterior chamber. Two commercial systems were selected for comparison, one a low resolution swept source (Tomey CASIA,

Tomey Corporation, Nagoya, Japan) and one of the highest resolution spectral domain systems currently available (Heidelberg Spectralis, Heidelberg Engineering, Heidelberg, GmbH).

2.4 Pharmaceutical pellets

To demonstrate applications to complex pharmaceutical coatings, a multi-layer pellet system was chosen. Pellets at three stages of the production process were sampled and imaged.

3. RESULTS

3.1 Spectrograph evaluation

Figure 3 compares the images of curved cling film taken using the three spectrographs. With the Czerny-Turner spectrograph, significant artefacts are present a significant distance in front of the semi-glossy surface reflections. With the application of FPDM, this artefact type is reduced (this is quantified in [16]) but some artefact still remains. For both the Schmidt-Czerny-Turner and transmission spectrographs, with much less imaging aberrations, none of this type of artefact could be identified in the images. However, as well as glossy films, we also found the smooth curved surface of lenses give significant artefacts. Figure 4 shows images of lenses taken with the Schmidt-Czerny-Turner and transmission spectrographs, though these removed the artefact type present in curved cling film imaging, significant distortion of the interface signal is seen, with the apparent splitting of specular and diffuse signal. Further investigation is required to identify the precise cause of this artefact.

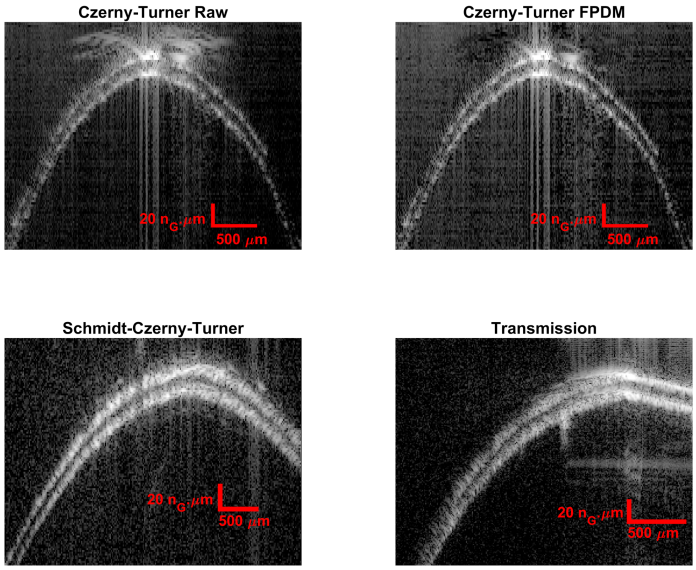

Figure 3. LF-OCT images of curved cling film taken using three different spectrograph setups: Top left Czerny-Turner Raw, top right Czerny-Turner with FPDM, bottom left Schmidt-Czerny-Turner, and bottom right transmission.

The specular or semi-specular reflecting samples above are not typical of real objects or tissue that is commonly the target for OCT, they serve only as a worst case scenario to study artefacts. To understand the impact optical imperfections have in real practice, images of a realistic diffusively scattering sample needs to be compared. Figure 5 gives the comparison images of the front of a fixed donor cornea taken with the three spectrograph setups. The increased image artefacts expected in the raw Czerny-Turner spectrograph are visible in front of the surface. However, overall there is little difference in the image quality between the three systems. This matches our observation throughout the project that though the Czerny-Turner spectrograph is optically flawed, there are no significant induced artefacts visible for most samples, particularly if FPDM is also applied. Though not ideal, a Czerny-Turner spectrograph is suitable for LF-OCT and provides instrument flexibility at a relatively low cost. Schmidt-Czerny-Turner spectrograph does overcome the Czerny-Turner imaging limitations, but does come at a higher cost and there other non-spectrograph optics

related artefacts which will still be present. Transmission spectrographs are low cost, less bulky and have the same imaging properties as Schmidt-Czerny-Turner, at the cost of removal of flexibility in setup.

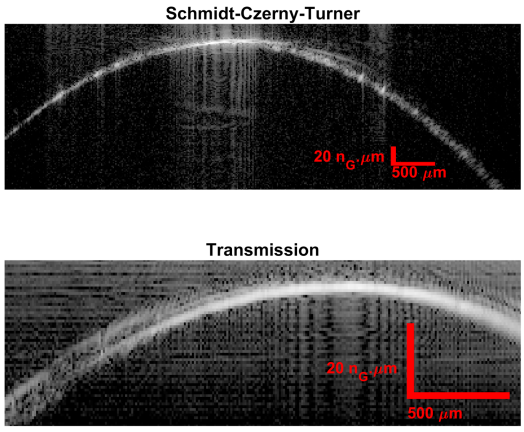

Figure 4. LF-OCT images of surface of lenses taken with Schmidt-Czerny-Turner (top) and transmission (bottom) spectrographs.

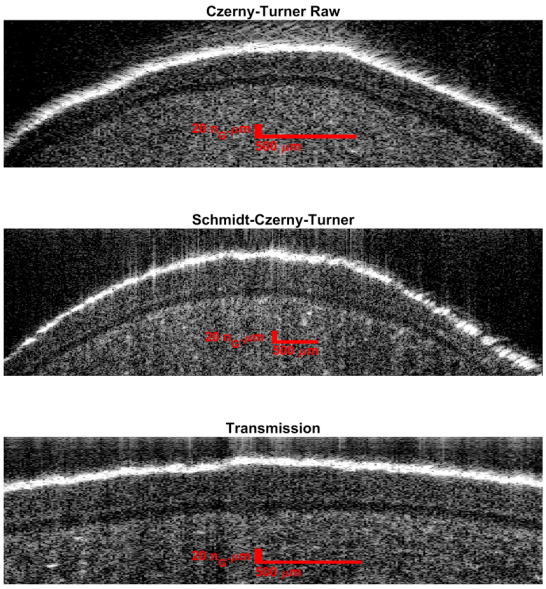

Figure 5. Images of the front of fixed cornea taken with Czerny-Turner (top), Schmidt-Czerny-Turner (middle) and transmission (bottom) spectrographs.

3.2 Human donor cornea comparison between UHR-LF-OCT and current commercial clinical OCT systems

We imaged human corneas *ex vivo to* demonstrate that the UHR-LF-OCT system, even with the optically imperfect Czerny-Turner imaging spectrograph, gives much improved image resolution and thus diagnostic potential compared with current clinical OCT systems.. Figure 6 shows comparable images of the same donor cornea, prepared to be at *in vivo* thickness, taken with a low axial resolution current commercial clinical system (Tomey Casia), a high resolution

current commercial clinical system (Heidleberg Spectralis) and our system. For the resolution of the layers, the differences between the systems are clear. The low resolution system barely resolves the epithelium from the stroma. The high resolution system resolves the epithelium and the location of the Bowman's layer is visualised, but probably not well enough to allow accurate measurement. At the posterior interface, both commercial systems show a strong signal from the endothelium, but would not be able to accurately resolve its thickness. The Descemet's membrane is not visible at all for both commercial systems. Our system has significantly better resolution, the epithelium and Bowman's layer are fully resolved and their thicknesses could be mapped accurately. Also, the Descemet's membrane and endothelium layers are resolved from each other. The signal from the stroma also highlights the massive resolution improvement. For the low resolution system the signal is just a speckle pattern with no structural information. For the high resolution system, some structural signals are apparent behind the speckle pattern. For our system, however, these structural features are clearly resolved and will be lamellae or keratocytes.

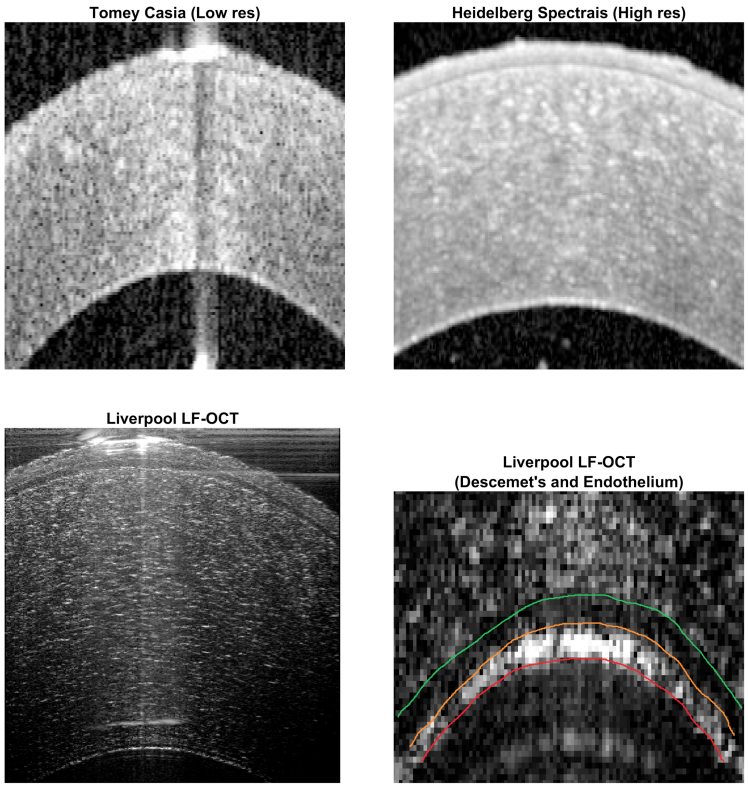

Figure 6. Images of human donor cornea taken with low (top left) and high (top right) current clinical OCT systems, and our UHR-LF (bottom left) OCT system. (Bottom Right) is an enlargement of Descemet's and endothelial layers in the UHR-LF OCT image, with stroma-Descemet's (green), Descemet's-endothelial (orange) and endothelial-medium (red) boundaries manual marked.

One significant apparent imaging illusion seen here and previous UHR[7,13] studies is that, while corneal volumes in non-UHR OCT images are filled by apparent signal (continuous white in the images), in UHR images corneal volume appear more sparse (images more black with white only at scattering points). It is likely that the total photon energies captured in the images are the same, but the axial blurring of the linear field (proportional to the square root of energy) image by non-UHR OCT that is then displayed logarithmical causes the apparent filled image. Though additional photon coherence gating effects by UHR is not ruled out.

3.3 Pharmaceutical pellets

Figure 7 shows UHR-LF-OCT images of pharmaceutical pellets with different numbers of coatings applied. The "un-coated" substrates already have a layered structure (boundaries marked in green), which maybe due to the core structure

or a prior coating. The addition of a transparent first (surface marked in red) and a scattering second (surface marked in orange) coatings are also identified. There has been recent research[8,9,20] into the use of OCT for in-line monitoring of pellet and tablet production, the addition of UHR allows thinner layers to be resolved and measured. We have previously demonstrated that a single super continuum pulse could be used in LF-OCT for ultra fast measurements[16], which would allow undistorted measurements of pellets or tablets in a tumble bed coater.

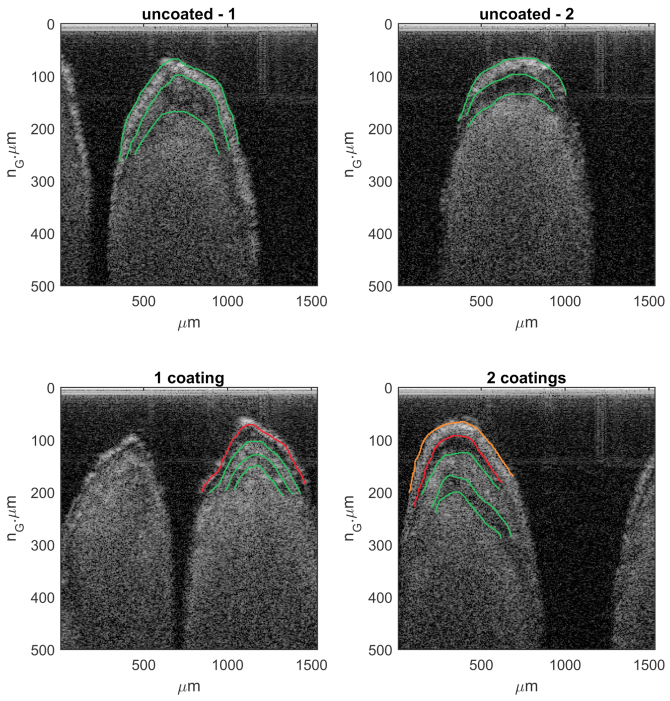

Figure 7. LF-OCT images of pellets at three stages of a multi-coat process. (Top left) and (top right) show the initial substrate used and pre-existing structure, (bottom left) after the addition of a first clear coating and (bottom right) after the addition of a second scattering coating.

4. CONCLUSION

Line-field (LF) spectral domain is a format of OCT that reduces the impact of the spectral Relative Intensity Noise (RIN) of suppercontinuum light sources. This is due to two mechanisms; firstly the parallel detection allows greater averaging of pulses without loss of imaging speed and secondly, with completely parallel detection, the spectral RIN is identical in all A-Scans so can be mathematically identified as fixed pattern noise and removed. The effect of imaging spectrograph design on optical crosstalk artefacts in LF-OCT was experimentally assessed, identifying one type of artefact caused by imaging aberrations of Czerny-Turner setup and one type of artefact independent of imaging spectrograph. However, for most real samples the effect of cross-talk is likely to be negligible, and here it was demonstrated that the benefits of ultra-high resolution (UHR), with even a Czerny-Turner based LF-OCT system, compared with current scanning point systems, dominates. In addition, the benefits of commercially viable UHR OCT can be extended to fields beyond medicine and here we present images of multi-layer pharmaceutical pellets as an example.

ACKNOWLEDGEMENTS

The Ultrasensitive Optical Coherence Tomography Imaging for Eye Disease is funded by the National Institute for Health Research's i4i Programme. This paper summarises independent research funded by the National Institute for Health Research (NIHR) under its i4i Programme (Grant Reference Number II-LA-0813-20005). The views expressed are those of the authors and not necessarily those of the NHS, the NIHR or the Department of Health. This work is also partially supported by UK EPSRC (EP/L019787/1).

REFERENCES

1. Huang, D. et al. Optical coherence tomography. Science 254, 1178-1181, doi:10.1126/science.1957169 (1991).
2. Fujimoto, J. & Swanson, E. The Development, Commercialization, and Impact of Optical Coherence Tomography. Invest. Ophthalmol. Vis. Sci. 57, OCT1-OCT13, doi:10.1167/iovs.16-19963 (2016).
3. Drexler, W. & Fujimoto, J. G. Optical Coherence Tomography: Technology and Applications. (Springer Berlin Heidelberg, 2008).
4. Stifter, D. Beyond biomedicine: a review of alternative applications and developments for optical coherence tomography. Applied Physics B-Lasers and Optics 88, 337-357, doi:10.1007/s00340-007-2743-2 (2007).
5. Drexler, W. et al. In vivo ultrahigh-resolution optical coherence tomography. Optics Letters 24, 1221-1223, doi:10.1364/ol.24.001221 (1999).
6. Vajzovic, L. M. et al. Ultra high-resolution anterior segment optical coherence tomography in the evaluation of anterior corneal dystrophies and degenerations. Ophthalmology 118, 1291-1296 (2011).
7. Werkmeister, R. M. et al. Ultrahigh-resolution OCT imaging of the human cornea. Biomedical Optics Express 8, 1221-1239 (2017).
8. Mauritz, J. M. A., Morrisby, R. S., Hutton, R. S., Legge, C. H. & Kaminski, C. F. Imaging Pharmaceutical Tablets with Optical Coherence Tomography. J. Pharm. Sci. 99, 385-391, doi:10.1002/jps.21844 (2010).
9. Li, C., Zeitler, J. A., Dong, Y. & Shen, Y.-C. Non-Destructive Evaluation of Polymer Coating Structures on Pharmaceutical Pellets Using Full-Field Optical Coherence Tomography. J. Pharm. Sci. 103, 161-166, doi:10.1002/jps.23764 (2014).
10. Fercher, A. F. et al. A thermal light source technique for optical coherence tomography. Opt. Commun. 185, 57-64, doi:10.1016/s0030-4018(00)00986-x (2000).
11. Wang, Z. et al. Cubic meter volume optical coherence tomography. Optica 3, 1496-1503, doi:10.1364/optica.3.001496 (2016).
12. Alfonso, R. R. (Springer, New York, 2006).
13. Yadav, R. et al. Micrometer axial resolution OCT for corneal imaging. Biomedical Optics Express 2, 3037-3046 (2011).
14. Kudlinski, A. & Mussot, A. Optimization of continuous-wave supercontinuum generation. Optical Fiber Technology 18, 322-326, doi:10.1016/j.yofte.2012.06.003 (2012).
15. Zuluaga, A. F. & Richards-Kortum, R. Spatially resolved spectral interferometry for determination of subsurface structure. Optics Letters 24, 519-521, doi:10.1364/ol.24.000519 (1999).
16. Lawman, S. et al. High resolution corneal and single pulse imaging with line field spectral domain optical coherence tomography. Opt. Express 24, 2395-2405, doi:10.1364/oe.24.012395 (2016).
17. McClure, J. P. The Schmidt-Czerny-Turner spectrograph in Conference on Photonic Innovations and Solutions for Complex Environments and Systems (PISCES) II. (Spie-Int Soc Optical Engineering, 2014).
18. Grajciar, B., Pircher, M., Fercher, A. F. & Leitgeb, R. A. Parallel Fourier domain optical coherence tomography for in vivo measurement of the human eye. Opt. Express 13, 1131-1137, doi:10.1364/opex.13.001131 (2005).
19. Zhang, Y., Rha, J. T., Jonnal, R. S. & Miller, D. T. Adaptive optics parallel spectral domain optical coherence tomography for imaging the living retina. Opt. Express 13, 4792-4811, doi:10.1364/opex.13.004792 (2005).
20. Markl, D. et al. Automated pharmaceutical tablet coating layer evaluation of optical coherence tomography images. Measurement Science and Technology 26, 035701, doi:10.1088/0957-0233/26/3/035701 (2015).